

JPL D-13913 (REVISED)

Advanced Spaceborne Thermal Emission & Reflection Radiometer



Algorithm Theoretical Basis Document for: **Brightness Temperature**

Version 3.0

April 5, 1999

Prepared by:
Ronald Alley, Jet Propulsion Laboratory
Marit Jentoft-Nilsen, Jet Propulsion Laboratory

Algorithm Theoretical Basis Document

for

Brightness Temperature

Version 3.0 April 5, 1999

Ronald E. Alley
Marit Jentoft-Nilsen
Jet Propulsion Laboratory
4800 Oak Grove Drive
Pasadena, CA 91109

1.0 Introduction

The Advanced Spaceborne Thermal Emission and Reflectance Radiometer (ASTER) is a high-spatial-resolution multispectral imaging device scheduled to fly in Earth orbit starting in mid-1999, on the first platform of NASA's Earth Observing System (EOS-AM1). The instrument will have three bands in the visible and near infrared (VNIR) spectral range (0.5 to 1.0 μm) with 15 meter spatial resolution, six bands in the short-wave infrared (SWIR) spectral range (1.0 to 2.5 μm) with 30 meter spatial resolution, and five bands in the thermal infrared (TIR) spectral range (8 to 12 μm), with 90 meter spatial resolution (Kahle, et al., 1991; Yamaguchi, et al., 1993). An additional backward viewing telescope with a single band in the near infrared with 15 meter spatial resolution will provide the capability, when combined with the nadir viewing elements, for same-orbit stereo data. The instrument is being provided by the Japanese Government under the Ministry of Trade and Industry (MITI). The ASTER project is implemented through the Earth Resources Satellite Data Analysis Center (ERSDAC) and the Japan Resources Observation System Organization (JAROS), which are nonprofit organizations under the control of MITI. JAROS is responsible for the design and development of the ASTER instrument, which will be carried out by the Nippon Electric Company (NEC), the Mitsubishi Electric Corporation (MELCO), Fujitsu, and Hitachi under contracts with JAROS. The ASTER science team is an international team of Japanese, American, French, and Australian scientists. The team participates in the definition of the scientific requirements for ASTER, in the development of algorithms for data reduction and analysis, and in calibration, validation, and mission planning.

1.1 Algorithm Identification

This Algorithm Theoretical Basis Document (ATBD) describes the algorithm to be used to produce the brightness temperature at sensor product (ASTER product number AST04). This product is currently scheduled to be produced only for TIR data, although the algorithm could be adapted for SWIR data nighttime scenes containing elevated temperatures.

1.2 Data Product Name and Number

Brightness Temperature at Sensor, product number AST04

1.3 Document Scope

The purpose of this document is to describe both the theoretical basis and practical aspects of the brightness temperature algorithm in sufficient detail to allow the ASTER science team and Algorithm Review Board to evaluate it. The document starts with a description of the general background of the algorithm and the basic equation defining the

relation between the input and output products. It then gives a detailed mathematical description of the algorithm used to solve the basic equation, including variance and uncertainty estimates. The final section discusses the practical and numerical considerations, including calibration and validation, programming considerations, diagnostics, exception handling, limitations, and assumptions. Included as an appendix is a chart of the ASTER Standard Product interdependencies.

2.0 Overview and Background Objective

2.1 Experimental Objective

ASTER is the only high spatial resolution surface imaging instrument on the EOS-AM1 platform. As a result, there are a variety of unique science objectives that the instrument will be able to address. The main contributions to the EOS global change studies will be in providing surface temperatures, surface emitted and reflected radiance, cloud properties, and digital elevation models (DEMs) at a spatial scale that will allow detailed studies to be conducted.

EOS AM-1 will carry two other surface imaging instruments in addition to ASTER. They are the Multi-angle Imaging Spectro-Radiometer (MISR) and the Moderate Resolution Imaging Spectrometer (MODIS). High spatial resolution data from ASTER will be used to create datasets on a spatial scale of tens of meters. This data can be verified by field measurements, which, at the same time can be used to understand the averaged response of the instruments that have coarser spatial resolution. ASTER can study in more detail those quantities and processes (such as the surface properties, elements of the surface energy and water balance, and cloud properties) that are monitored globally by MODIS and/or MISR at a moderate resolution. Data from MODIS and MISR will be used to help with the atmospheric correction of ASTER data.

The objective of the algorithm described in this document is to convert the radiance values that have been observed by the sensor into the corresponding brightness temperature values. The brightness temperature product contains essentially the same information as the input radiance product, but in a form that is more easily and intuitively understood. Temperature units are almost universally familiar, while only a fraction of the potential user community has an intuitive grasp of radiance units.

Spectral emissivity variations are also more apparent in the brightness temperature product than in the radiance product. Since a particular pixel has a kinetic temperature, independent of wavelength, the deviations of the brightness temperature from band to band may be ascribed to spectral emissivity differences. The spectral emissivity curve for a pixel is essentially the inverse of the brightness temperature curve. The user can therefore readily find features of spectral emissivity by inspection of the brightness temperature values.

2.2 Historical Perspective

The radiance perceived by a sensor is a function of the radiation emitted from the target and the radiation emitted and absorbed by the intervening atmosphere, integrated over the response function of the sensor. The radiation emitted from the target at a given wavelength is a function of its temperature and emissivity. Atmospheric effects are disregarded in the calculation of brightness temperature at the sensor, so we can say the radiance at the sensor is the integral over the instrument response function of the emissivity times the blackbody radiance. The temperature and the spectral emissivity are the unknowns in this equation. If we set the emissivity to one, we can calculate the remaining unknown, the temperature. Setting the emissivity to one is equivalent to assuming that the target is a blackbody, so the brightness temperature can be defined as the temperature that a blackbody would be in order to produce the radiance perceived by the sensor. Brightness temperature has been used to observe volcanic ash clouds (Prata, 1989) and detect ice leads in the Arctic (Stone, 1993) to name just a few examples.

2.3 Instrument Characteristics

ASTER will provide data in three spectral regions using three separate radiometer subsystems. These are the visible and near-infrared (VNIR) subsystem being provided by NEC, the short wavelength infrared (SWIR) subsystem provided by MELCO, and the thermal infrared (TIR) subsystem provided by Fujitsu. The instrument bandpasses, radiometric accuracy, and radiometric and spatial resolution for the TIR and SWIR subsystems are given in Table 1. A wide dynamic range and multiple gain settings will help ensure useful data for a variety of investigations. Current plans call for only TIR data to be used for input into the brightness temperature algorithm, although the algorithm could be expanded to include nighttime SWIR data at some future date.

The swath width is 60 kilometers for each of the three subsystems. The ASTER instrument has a crosstrack pointing capability of 8.55 degrees for the TIR and SWIR subsystems, which gives a crosstrack observational range of approximately 136 kilometers on the surface. Any point on the earth's surface (except the extreme polar regions) will be accessible by the TIR and SWIR at least once every sixteen days.

Instrument and spacecraft resources are allocated to support an eight percent average duty cycle, which corresponds to over 700 60x60 kilometer scenes per day. ASTER data will be acquired and processed according to specific user requirements that identify the acquisition time, gain, wavelength region, and data product. In addition, ASTER has the goal of obtaining a cloud-free data set for the entire Earth's land surface by the end of its mission. Users will be able to request that data

products, of local and regional extent, be made from the global data set. The stereo capability will be used to generate high resolution digital elevation models (DEMs) in selected regions. Observations will also include sites involving highly coordinated field experiments with simultaneous ground and aircraft measurements, targets of opportunity such as volcanoes, fires and major weather events, and observations of clouds on a local to regional scale.

Table 1. Spectral and spatial characteristics of the ASTER TIR and SWIR instruments.

ASTER TIR and SWIR					
Wavelength Region	Band Number	Spectral Range (μ m)	Radiometric Accuracy	Radiometric Resolution	Spatial Resolution
SWIR	4	1.60-1.70	$\pm 4 \%$	$\leq 0.5 \%$	30 m
	5	2.145-2.185	$\pm 4 \%$	$\leq 1.3 \%$	30 m
	6	2.185-2.225	$\pm 4 \%$	$\leq 1.3 \%$	30 m
	7	2.235-2.285	$\pm 4 \%$	$\leq 1.3 \%$	30 m
	8	2.295-2.365	$\pm 4 \%$	$\leq 1.0 \%$	30 m
	9	2.360-2.430	$\pm 4 \%$	$\leq 1.3 \%$	30 m
TIR	10	8.125-8.475	1-3 _K	$\leq 0.3 \text{ _K}$	90 m
	11	8.475-8.825	1-3 _K	$\leq 0.3 \text{ _K}$	90 m
	12	8.925-9.275	1-3 _K	$\leq 0.3 \text{ _K}$	90 m
	13	10.25-10.95	1-3 _K	$\leq 0.3 \text{ _K}$	90 m
	14	10.95-11.65	1-3 _K	$\leq 0.3 \text{ _K}$	90 m

3 Algorithm Description

3.1 Theoretical Description

3.1.1 Physics of the Problem

The spectral radiance of a blackbody at temperature, T , and wavelength, λ , is given by the Planck function.

$$L_{\lambda}^{BB} = \frac{C_1}{\lambda^5 \pi \left[e^{\frac{C_2}{\lambda T}} - 1 \right]} \quad (1)$$

where:

- L^{BB} = blackbody radiance ($\text{W-m}^{-2}\text{-steradian}^{-1}\text{-}\lambda^{-1}$)
- λ = wavelength (m)
- T = temperature (K)
- C_1 = first radiation constant ($3.74151 \times 10^{-22} \text{ W-m}^3\text{-}\lambda^{-1}$)
- C_2 = second radiation constant (0.0143879 m-K)

This equation is integrated over an instrument response function to calculate the radiance that corresponds to a brightness temperature for a particular instrument channel (band).

$$L_s = \frac{\int \psi(\lambda) L^{BB}(T, \lambda) d\lambda}{\int \psi(\lambda) d\lambda} \quad (2)$$

where:

- L_s = radiance observed by the sensor
- ψ = instrument response

A mathematical description of the technique to solve for temperature is provided below.

3.1.2 Mathematical Description of Algorithm Alternatives

The solution that we seek is the inverse of Equation 2. That is, we wish to compute temperature (T) as a function of sensor radiance (L_s).

Unfortunately, for sensor response functions of finite (not infinitesimal) width, Equation 2 cannot be inverted explicitly. Several methods have been examined to approximate the solution of the inverse of Equation 2.

The most straightforward approximation is to replace the response function with a delta function at the sensor's central wavelength. Under this approximation Equation 2 collapses into Equation 1, which can be inverted to

$$T_c = \frac{c_2}{\lambda_c \log \left(\frac{c_1}{\lambda_c^5 \pi L_s} + 1 \right)} \quad (3)$$

where:

T_c = brightness temperature, from a central wavelength
 λ_c = the sensor's central wavelength

Implicit in the computation of a central wavelength for a TIR sensor is a standard temperature. Equation 3 is accurate for the observed radiance that yields the standard temperature, but it becomes increasingly inaccurate for temperatures farther away from the standard temperature.

Also considered was an alternative method that uses the result of the preceding technique as a first guess at the solution. The computed temperature is used to solve the right-hand side of Equation 2. For a set of calibrated sensor response values, Equation 2 becomes

$$L_c = \frac{\sum_i \psi_i \cdot L^{BB}(T_c, \lambda_i) \cdot \Delta \lambda}{\sum_i \psi_i \cdot \Delta \lambda} \quad (4)$$

where

L_c = computed radiance from the trial temperature

This computed radiance should ideally be equal to the observed sensor radiance. By adjusting the trial temperature in Equation 4, an iterative method can be established, which will converge upon the solution to any desired precision. This approach is, however, computationally time consuming.

The first method was ultimately rejected because of its inaccuracy. Variations of the second method were rejected on the basis of their computational demands.

3.1.3 Mathematical Description of the Algorithm

The algorithm that has been selected does not attempt an inversion of Equation 2 by making a simplifying approximation. Instead, Equation 2 is solved directly; the expected radiance at the sensor is computed at finely spaced temperature intervals for the range of temperatures that

the sensor is designed to receive. This results in a table of values that represent observed radiance as a function of brightness temperature for a given sensor. Rather than invert Equation 2, we invert the generated table (that is, form a new table from the old one, where brightness temperature is represented as a function of observed radiance). It is possible to invert this table to any desired precision by simply enlarging the original table to include a sufficient number of entries in the table. The generation and inversion of this table are computationally expensive, but the results are constant for a given wavelength calibration of the sensors, and therefore, presumably, for the life of the mission. The table need be generated and inverted only once, prior to launch. Then, to generate the brightness temperature product for a given scene, one need only use the radiance value of each input pixel as the index to point to the desired brightness temperature in the stored table, and place the table values in the output dataset.

It would be instructive to show in detail how this table is generated and inverted. Doing this will not only clarify the technique used, but it will also illuminate the constraints that are needed to maintain precision.

The input dataset for this product is the radiance observed at the sensor, in units of Watts per square meter per steradian per micrometer. The input values are stored as sixteen bit signed integer, meaning that (1) there is a maximum of 65,536 (2^{16}) distinct input values, and (2) a scaling factor (perhaps with an offset, also) will be needed to convert the stored values into the specified units. As of this writing, the scaling factor had not been determined. For the purposes of this example, a scaling factor of 1000, with no offset is assumed. Such a scaling factor would imply data values between 500 and 28,500 in all TIR channels for temperatures between 200 and 370 degrees Kelvin, the design range for the TIR subsystem. The chosen scaling factor could differ by approximately a factor of two in either direction before either the radiance calibration begins to noticeably degrade, or unsaturated pixels become saturated during the calibration process.

The output product is reported in units of degrees Celsius, scaled by a factor of 100. For example, an output value of 2735 implies a brightness temperature of 27.35 degrees. Since the brightness temperature values are stored as 16 bit signed integers, the precision of the brightness temperature values will be 0.01 degrees Celsius. Like the input, output values are stored as sixteen bit signed integers, permitting 65,536 possible output values.

To construct the table of radiance values as a function of brightness temperature and ASTER channel, Equation 4 is solved for the temperature values that span the range of possible observed radiance

values. The temperature values used will be in 0.010 degree increments, starting with -200.00 degrees Celsius, and increasing to +200.00 degrees Celsius. (The choice of limits as -150 to +200 degrees is fairly arbitrary and may be adjusted. The important criterion is that the limits are certain to extend beyond the range of temperatures that ASTER will be able to detect. The range -150 to +200 meets this criterion.) The computed values represent the bounding values of radiance that correspond to each possible output temperature value.

To invert the table just described, each of the 2^{16} possible input radiance values is compared to the table values. Each radiance value will fall between two of the table entries; that radiance is then assigned that temperature (to the nearest 0.01 degree) that also falls between those two entries. The resulting table will contain 2^{16} by 5 entries, with each entry a value that represents the temperature corresponding to that radiance and channel. The associated radiance values are implied by the location of each table entry. The table is permanently stored for later use in generating the brightness temperature product.

When a brightness temperature product needs to be generated, the task is simply a matter of table lookup. The input value of each pixel is used as an index to a location in the table. The output value for that pixel is the content of that location.

3.1.4 Variance and Uncertainty Estimates

The uncertainties introduced by this algorithm result from two sources: errors and uncertainties in the wavelength calibration of the instrument, and the rounding (digitization) error imposed by the method of storing the results.

The rounding errors should be uniformly distributed over the range ± 0.005 degrees Celsius, yielding a standard deviation of 0.0029 degrees. The ASTER TIR design specification does not require a radiometric resolution better than 0.3 degrees. For a perfectly linear radiometric response over the specified temperature range for ASTER TIR, the 12 bit recording level of the instrument limits the resolution to no better than 0.02 degrees, under any conditions.

A full assessment of the uncertainties of the wavelength calibration must await the actual calibration, but a few general comments can be stated now. The brightness temperature results will be fairly insensitive to random errors (errors in the shape of the response function), but more sensitive to any bias (errors in the central wavelength value). As a crude rule of thumb, a 5 nanometer error in the central wavelength is required to produce a 0.02 degree error in the calculated brightness temperature.

The wavelength calibration is not expected to be a major source of error (uncertainty) in the results of this product.

In conclusion, it is assumed that the largest source of uncertainty in the output values will be the corresponding uncertainty of the input values.

3.2 Practical Considerations

3.2.1 Numerical Computation Considerations

By creating a table that can be used to process all scenes, the time consuming computations are moved from the post-launch data product generation to the pre-launch software development. Using this method will result in a substantial saving in the operational software execution time.

The size of the lookup table will be no larger than 32,768 entries (2^{16} entries per channel * 5 channels). The table may, in fact, be smaller. For example, if the scaling factor for the data is chosen to be 1000, with no offset (the values used in the example of Section 3.1.3), all negative input values would correspond to negative radiance values. Since these values physically unrealistic, no table entries need be provided for them, and the table size could be cut in half. Even under the worst circumstances, this table can be easily held in memory during the program execution.

3.2.2 Programming / Procedural Considerations

The radiance to temperature lookup table is presently envisioned as a separate file, to be read by the brightness temperature software each time an ASTER brightness temperature product is generated. Alternatively, the lookup table could be included as part of the program software itself. This would result in a slight gain of execution speed, at a small cost to the clarity of the software. This alternative is not expected to be used unless program execution speed becomes an overwhelming issue.

The software delivery for this product will include the lookup table, rather than the software to generate the lookup table.

This approach is well suited to potential parallel processing implementations, since the lookup on each pixel is independent of any other pixel's value.

3.2.3 Calibration and Validation

The output temperature value for a pixel depends upon two values, the input radiance value, and the sensor spectral response function. The

radiance calibration is discussed in the ATBD for the Level 1B product, "Radiance at Sensor - TIR". The pre-launch calibration of the sensor spectral response functions will be carried out by Fujitsu, the manufacturer of the TIR subsystem. A full post-launch verification of the pre-launch calibration is not feasible, but the ASTER data acquired for post-launch validation of the Level 1B product will be examined to verify that it is consistent with the pre-launch calibration.

The primary validation concern for this product is one of software testing. Has the lookup table been constructed properly, and does the associated computer program manipulate the input data and the lookup table correctly? To assure proper operation, the brightness temperature product will be generated for a scene of ASTER simulated data. The results will be compared to results obtained from independently created software, software that does not use the lookup table associated with the brightness temperature product software.

3.2.4 Quality Control and Diagnostic Information

Quality control on this product will more an assessment of the input data (radiance products and the instrument response functions used to calculate the lookup table) than of the algorithm itself. The quality control and diagnostic information that will be produced and appended to this product consists of a histogram of the brightness temperature values (1 _C intervals with a range -100 to +100 _C).

In addition, all ASTER Level 2 products will contain a pixel map in a format common to all of the products. This map will identify any pixels which are known to be defective, and report the nature and severity of the defect. The map will also note the presence of clouds in the pixel, to the extent that this information is known.

3.2.5 Exception Handling

No attempt will be made to calculate the brightness temperature for pixels that have been previously identified as:

- 1) Dropped lines
- 2) Dropped pixels
- 3) Invalid data

These values will be replaced with a predetermined replacement value for "bad" pixels.

4.0 Constraints, Limitations, Assumptions

At present there are no known constraints on the algorithm that would prevent it from producing a valid output product from any valid input thermal radiance image.

The conversion from radiance to temperature is performed only upon those pixels for which the input radiance is a positive value. All other pixels will be marked upon output as invalid data.

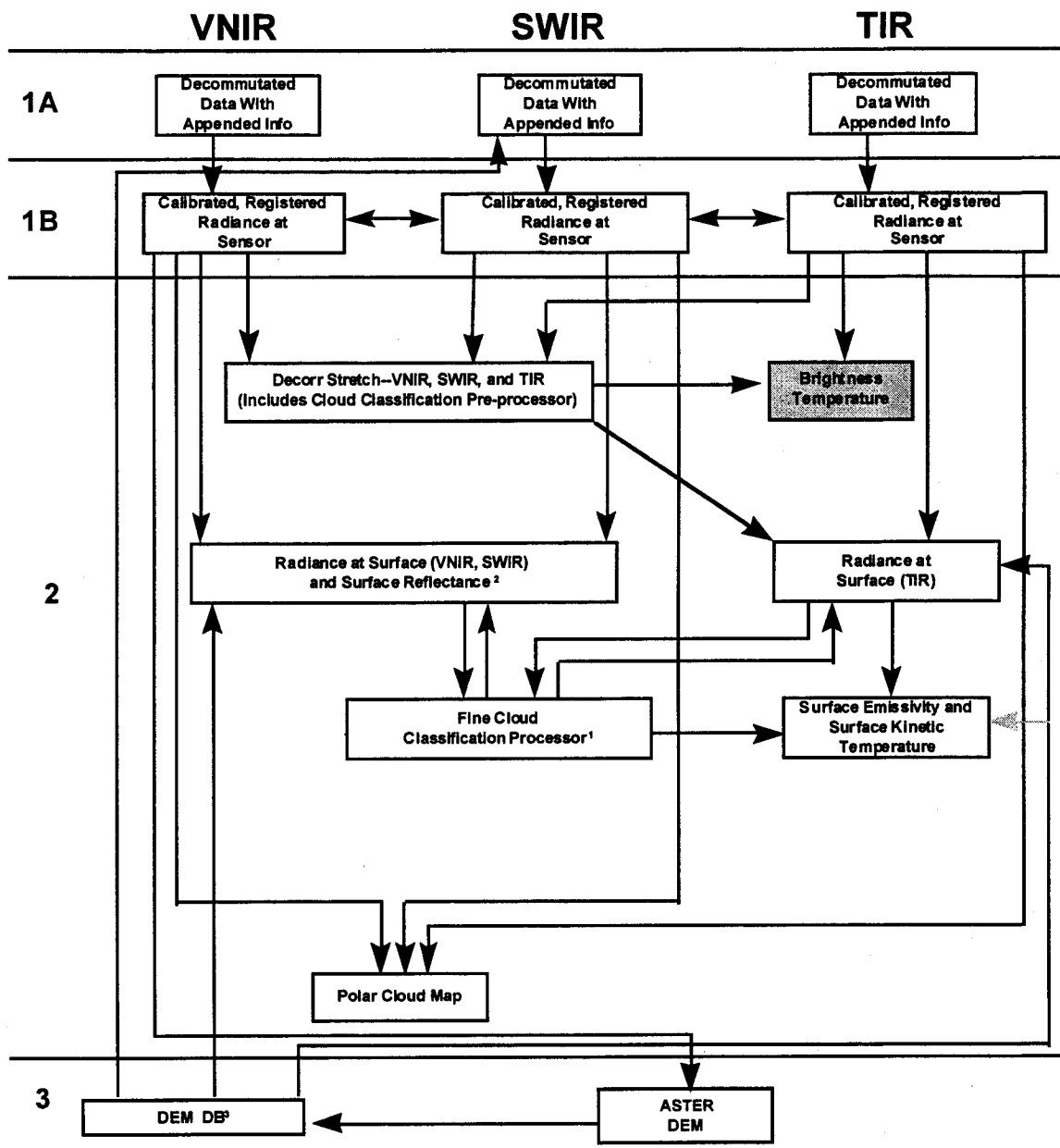
The algorithm is based upon the assumption that the ASTER TIR subsystem will have a complete sensor response calibration performed prior to launch, and that the results of that calibration will be made available to the implementors.

Brightness temperature is defined as the temperature that a blackbody would have in order to produce the observed radiance. If one considers a brightness temperature to be the surface temperature, that person has assumed that the atmospheric path has had no effect on the radiance value, and that the surface is emitting as a blackbody (i.e., with a spectral emissivity of 1.0 at all wavelengths).

5.0 References

- Fujisada, H., and Ono, A. 1993. Anticipated performance of the ASTER instrument in EM design phase. *SPIE Proceedings*. pp. 187-197.
- Kahle, A. B., Madura, D. P., and Soha, J. M. 1980. Middle Infrared Multispectral Aircraft Scanner Data Analysis for Geological Applications. *Applied Optics*, vol. 19, pp. 2279-90.
- Kahle, A. B., Palluconi, F. D., Hook, S. J., Realmuto, V. J., and Bothwell, G. 1991. The Advanced Spaceborne Thermal Emission and Reflectance Radiometer (ASTER), *International Journal of Imaging Systems and Technology*, vol. 3, pp. 144-156.
- Palluconi, F. D., and Meeks, G. R., 1985. *Thermal Infrared Multispectral Scanner (TIMS): An Investigator's Guide to the Data*, JPL Publication 85-32.
- Planck, M. 1901. On the Distribution of Energy in the Spectrum. *Ann. Phys.*, vol. 4, no. 3, pp. 553-563.
- Prata, A. J. 1989. Observations of volcanic ash clouds in the 10-12 μ m window using AVHRR/2 data. *International Journal of Remote Sensing*, vol. 10, nos. 4 and 5, pp. 751-761.
- Sabins, Jr, F. F. 1978. *Remote Sensing Principles and Interpretation*. W. H. Freeman and Company, San Francisco, 426p.
- Siegal, R. and Howell, J. R. 1982. *Thermal Radiation Heat Transfer: Second Edition*, Hemisphere Publishing Corporation, New York.
- Stone, R. S. 1993. The Detectability of Arctic Leads using Thermal Imagery under varying Atmospheric Conditions. *Journal of Geophysical Research - Oceans*, vol. 98, no. nc7, pp. 12469-12482.
- Yamaguchi, Y., Tsu, H., and Fujisada, H. (1993). A scientific basis of ASTER instrument design. *SPIE Proceedings*, pp 150-160

ASTER Product Inter-Dependencies



¹Produces a cloud mask that is incorporated into other products

²Computed simultaneously with Radiance at Surface

³Refers to a database of DEM data regardless of the source